

CARBON ATMOSPHERIC TRACER RESEARCH TO IMPROVE NUMERICAL SCHEMES AND EVALUATION



CATRINE

Carbon Atmospheric Tracer
Research to Improve
Numerics and Evaluation

D3.1 Intercomparison Protocols in WP3-4

Due date of deliverable	December 2024
Submission date	December 2024
File Name	CATRINE-D3-1-V1
Work Package /Task	WP3
Organisation Responsible of Deliverable	WU
Author name(s)	WUR: Anja Raznjevic, Bart van Stratum, Maarten Krol UH: Leena Järvi URCA: Alohotsy Rafalimanana, Thomas Lauvaux, Charbel Abdallah
Revision number	1
Status	Issued
Dissemination Level / location	Public



Funded by the
European Union

The CATRINE project (grant agreement No 101135000) is funded by the European Union.

Views and opinions expressed are however those of the author(s) only and do not necessarily reflect those of the European Union or the Commission. Neither the European Union nor the granting authority can be held responsible for them.

1 Executive Summary

The CATRINE project aims to improve the accuracy of atmospheric tracer transport models. In the scope of that goal, high-resolution large-eddy simulations (LES) models will be employed to tackle the challenges of simulating greenhouse gas emissions from point sources and urban agglomerations. To this end, an intercomparison of multiple high-resolution models (MicroHH, PALM, WRF-LES) will be performed. The models will simulate the distribution of greenhouse gases (CO_2 , CH_4) and potentially co-emitted species (NO_x , CO ...) over several cities world-wide and evaluate simulated distributions to city-scale observations. Next to an evaluation of the simulations with available observations from ground stations, satellites, aircraft, and total columns, the simulated meteorology will be evaluated. These simulations will form the basis for recommendations on the added value of high-resolution simulations and emission quantification from hot-spot areas.

This document provides descriptions of the proposed benchmark simulations, the participating models, the boundary conditions, and the available observations for the evaluation. This protocol is intended as a living document, to which new protocols can be added. Currently, we focus on two cities: Rotterdam and Paris.

Table of Contents

1	Executive Summary	2
2	Introduction	4
2.1	Background.....	4
2.2	Scope of this deliverable	4
2.2.1	Objectives of this deliverables.....	4
2.2.2	Work performed in this deliverable	4
2.2.3	Deviations and counter measures.....	4
2.3	Project partners:	5
3	Models	6
3.1	MicroHH.....	6
3.2	WRF-LES	6
3.3	PALM model system	7
4	Case Studies	9
4.1	General notes	9
4.2	Rotterdam.....	9
4.2.1	Emissions	14
4.2.2	Validation datasets	14
4.3	Paris	17
4.3.1	Simulation configurations.....	17
4.3.2	Validation datasets	20
5	Simulation protocol	24
5.1	Data output	24
5.2	Non-standard data output	25
6	Appendix A (Rotterdam).....	26
A.1	Land surface	26
A.2	Air quality stations	26
7	References	29

2 Introduction

2.1 Background

The main objective of the Carbon Atmospheric Tracer Research to Improve Numerical schemes and Evaluation (CATRINE) project is to evaluate and improve numerical schemes for tracer transport in the new Copernicus anthropogenic CO₂ emissions Monitoring and Verification support capacity (CO2MVS) and the Copernicus Atmosphere Monitoring Service (CAMS).

Tracer transport modelling is at the core of the CO2MVS inversion system, since it links the anthropogenic emissions to observations of CO₂ and other tracers. However, incomplete knowledge of natural fluxes and random and systematic errors in the transport model will lead to errors in emissions estimations through inverse modelling (e.g., Schuh et al., 2019). This is a known issue (e.g. Lin and Gerbig, 2005) that is thought to be the main cause for the spread of the different flux inversions (Basu et al., 2018, Gaubert et al., 2019).

Currently, global GHG flux inversion systems are operating at maximum resolutions of ~1 degree, with efforts underway (e.g. CAMS) on performing simulations at resolutions of ~10 km. However, even this resolution might not be sufficient to properly link emissions from hot spots (such as cities) to atmospheric observations. Therefore, WP3 and WP4 of CATRINE aim to employ high-resolution models (Large-Eddy Simulations, LES) to link GHG emissions of cities and large point sources to atmospheric observations, and to quantify the representation and aggregation errors when assimilating satellite XCO₂ images into coarse-resolution inversion systems. To quantify the uncertainty in these high-resolution simulations, multiple models (WRF-LES, MicroHH, PALM) will be used to simulate the transport of GHG emissions in several urban environments. Moreover, output from the high-resolution simulations of the IFS system will be included in the comparison.

The first step in ensuring that the transport in these models is well represented is to benchmark these models against observations. This intercomparison protocol will ensure that all the models are run under the same conditions (e.g. simulation domain, resolution, boundary conditions, simulation period, ...) and are delivering their output in a standardized manner.

2.2 Scope of this deliverable

2.2.1 Objectives of this deliverables

The main objectives of this deliverable are to: (1) describe the participating models (2) document all case studies and requested simulation periods, (3) describe the input data available as boundary conditions, (4) list the observations that are available for model evaluation, (5) describe the required output and output format.

2.2.2 Work performed in this deliverable

This document lists and describes participating models, cities for which simulations will be performed, available input as well as validation datasets. Moreover, this protocol describes the output format in which the simulation results need to be delivered.

2.2.3 Deviations and counter measures

None.

2.3 Project partners:

Partners	
EUROPEAN CENTRE FOR MEDIUM-RANGE WEATHER FORECASTS	ECMWF
COMMISSARIAT A L ENERGIE ATOMIQUE ET AUX ENERGIES ALTERNATIVES	CEA
METEO-FRANCE	METEO-FRANCE
WAGENINGEN UNIVERSITY	WU
KARLSRUHER INSTITUT FUER TECHNOLOGIE	KIT
HELSINGIN YLIOPISTO	UH
UNIVERSITE DE REIMS CHAMPAGNE-ARDENNE	URCA
ALBERT-LUDWIGS-UNIVERSITAET FREIBURG	UFR

3 Models

3.1 MicroHH

MicroHH is a fluid dynamics code designed to perform direct numerical simulations (DNS) and large-eddy simulations (LES) in either idealized theoretical settings or realistic atmosphere (as described in van Heerwaarden et al. (2017)). The realistic atmosphere simulations are achieved by coupling MicroHH with ERA5 reanalysis data (Hersbach et al. 2020) data by using the Large-eddy simulation and Single column model – Large-Scale Dynamics ((LS)²D) Python package developed by van Stratum et al. (2023). MicroHH is capable of simulating both scalar and reactive plumes. The code is freely available on GitHub and can be downloaded following the instructions on the projects [Read the Docs site](#).

Large-eddy simulations have been implemented in MicroHH using a surface model that has been constrained to rough surfaces and large Reynolds numbers which is representative of typical atmospheric flows. The model estimates surface fluxes of momentum and scalar components using the Monin-Obukhov similarity theory (MOST, e.g. Stull, 2012). To quantify sub-grid kinematic momentum flux tensor MicroHH uses the Smagorinsky-Lily model (Lily, 1996, van Heerwaarden, 2017). Transport of scalars is solved with the advection-diffusion equation. For the reactive species, chemistry in the model is solved using a condensed chemistry scheme which is based on the scheme implemented in the CAMS/IFS (Inness et al., 2019, Krol et al., 2024).

Plume dispersion from point sources in MicroHH LES has been validated against wind tunnel experiments (Nironi et al., 2015) for a neutral channel flow by Ražnjević et al. (2022)a. It has also been used by Ražnjević et al. (2022)b to simulate methane plume dispersion from a point source in a realistic atmosphere. There, a measurement day during a campaign in Romania has been simulated with realistic meteorology boundary conditions. More recently, Krol et al., (2024) have used MicroHH to simulate chemically active NO_x plumes from various large point sources which were then evaluated against TROPOMI measurements.

3.2 WRF-LES

The Weather Research and Forecasting (WRF) model (Skamarock et al, 2008, 2019, <https://github.com/wrf-model/WRF>) is a widely used numerical weather prediction and atmospheric simulation tool, designed to address a range of meteorological and environmental studies. WRF's high-resolution capabilities, robust physics parameterizations, and flexibility make it a critical component for urban greenhouse gas (GHG) emission simulations. The WRF model has been widely utilized in numerous studies investigating greenhouse gas (GHG) emissions, demonstrating its significant potential to accurately simulate GHG concentrations and their spatial-temporal distribution. Its ability to incorporate detailed atmospheric processes and fine-scale spatial resolutions allows for a comprehensive understanding of emission sources and transport mechanisms of GHGs. Previous studies have shown that the WRF model is particularly effective in simulating the dispersion of GHGs at regional scales (Lauvaux T., et al. 2016; Gaudet, et al., 2017; Matthäus Kiel et al., 2021; Chulakadabba et al. 2023; Alexandre Danjou et al., 2024).

WRF-GHG (Beck et al., 2012) in the WRF-Chem model simulates CO₂, CH₄, and CO as passive tracers, focusing on transport and mixing without chemistry or removal processes. These gases are categorized into background, anthropogenic, and biomass burning tracers,

CATRINE

with fluxes from external inventories. Biogenic CO₂ fluxes are calculated using the VPRM model.

Vegetation Photosynthesis and Respiration Model (VPRM) (Mahadevan et al., 2008): This module is coupled with WRF to simulate biospheric CO₂ fluxes. It uses satellite data, such as Enhanced Vegetation Index (EVI) and Land Surface Water Index (LSWI), along with meteorological parameters, to model photosynthesis and respiration processes. This allows the inclusion of natural CO₂ fluxes in simulations alongside anthropogenic sources.

WRF-Chem Boundary Conditions (WRF-ChemBC): To simulate the transport and dispersion of tracers accurately, WRF integrates real-world boundary data from global models (e.g., CAMS) to ensure realistic lateral boundary conditions.

WRF-LES mode

The Large Eddy Simulation (LES) mode in WRF is designed for high-resolution simulations with grid spacings $\ll 1$ km, explicitly resolving turbulence and eddies at fine scales. LES is particularly effective for grid resolutions up to about 100 m. This resolution is crucial for simulating the complex turbulence structures and flows in environments such as urban areas. While WRF Planetary Boundary Layer (PBL) schemes are suited for grid resolutions greater than 1 km, LES explicitly resolves the major eddies, enabling 3-D turbulence schemes to handle sub-grid mixing. This allows LES to capture critical processes in urban settings, such as tracer (CO₂ or CH₄, ...) dispersion, influenced by buildings and streets, urban heat islands, and complex urban flows. However, the grid spacings between 200 m and 1 km is considered as a grey zone (Figure 3.1), where neither PBL and LES assumptions are perfect.

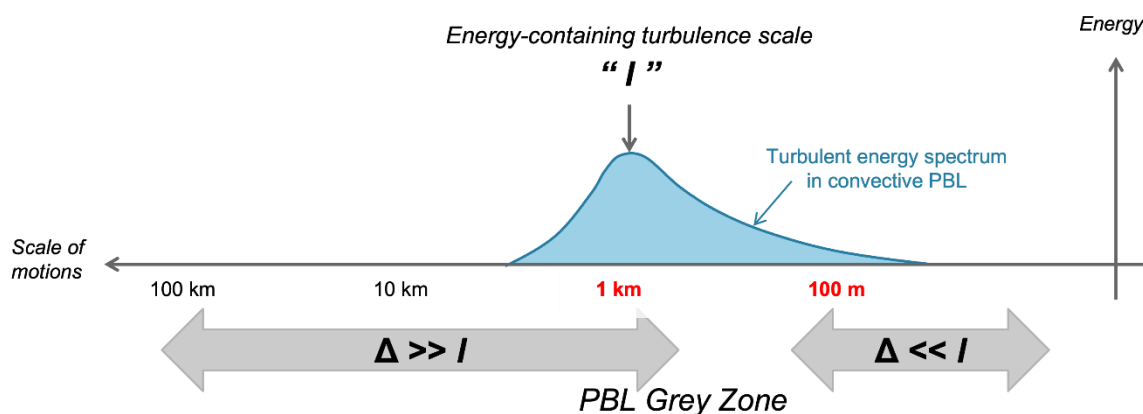


Figure 3.1: Model grid spacing, PBL and LES

3.3 PALM model system

The PALM model system (Maronga et al., 2020) has an LES core for atmospheric and oceanic boundary layer flows, which solves the non-hydrostatic, filtered, incompressible Navier–Stokes equations of wind (u , v , and w) and scalar variables in Boussinesq-approximated form on a staggered Cartesian Arakawa-C grid. Subgrid-scale turbulence is parameterised via the 1.5-order Deardorff scheme (Deardorff, 1980), and the momentum variables and scalars are discretized by the fifth-order advection scheme of Wicker and Skamarock (2002) together with the third-order Runge-Kutta time-stepping scheme (Williamson, 1980). PALM has been designed to run efficiently on parallel supercomputers, and it is thus exceptionally well-suited for high-resolution simulations. PALM contains an option for full three-dimensional two-way nesting (Hellsten et al., 2021) which enables to have both a large computational domain, and high spatial and temporal resolution in the main study area without making the simulation

CATRINE

computationally too expensive. PALM has land and urban surface models to solve the energy balance for each surface (Resler et al., 2017). These require the use of a radiation scheme RTM which calculates multiple reflections, diffuse radiation and absorbed radiation on different surfaces (Krč et al., 2021). PALM has also a plant canopy model which is used to model the interaction between vegetation and flow (Karttunen et al., 2020), a chemistry module (**Khan et al.**, 2021) and a Sectional Aerosol module for Large Scale Systems (SALSA) to solve the aerosol processes responsible for modifying the size distribution and pollutant interaction with the surface (Kurppa et al. 2019). In CATRINE, only passive scalars to describe carbon dioxide will be modelled. The PALM model system has been extensively evaluated against wind tunnel simulations showing good agreement for the mean flow and turbulence (Letzel et al., 2008; Razak et al., 2013; Kanani et al., 2014; Gronemeier and Sühling, 2019) and scalar dispersion (Park et al., 2012) within and above urban-like surfaces. The code is freely available.

4 Case Studies

Table 4.1 provides an overview of selected case studies and their simulation periods. The column Simulation days indicates the mandatory target days and Simulation period indicates the (optional) period for which to perform longer simulations. The case studies and simulation period were chosen based on the availability of observational data as will be detailed for the various cases below.

Table 4.1 Overview of case studies and simulation periods.

Case identifier	Case description	Mandatory simulation days	Simulation period (optional)
ROTT	RITA2022 ^(a)	23.08.2022 (ENE plume) 02.09.2022 (W plume)	22.08.2022 – 02.09.2022
PARIS	Paris & Île-de-France ^(b)	10.01.2024 – 20.01.2024	01.09.2023 – 11.09.2023

^(a) Campaign Rotterdam, focusing on emissions from harbor and city center.

^(b) Cases were selected based on the availability of observational data to evaluate the simulations. We have LIDAR data for the wind profile, along with measurements from several stations, including EM27, TCCON, and a network of CO₂ monitoring stations.

4.1 General notes

All simulations will be conducted using high-resolution models, which require specification of initial and time varying boundary conditions, dependent on the model set-up. For meteorological forcing it is recommended to use ERA5 data. Depending on the model configuration (e.g. nesting domains) other boundary conditions may be used. For greenhouse gases and chemical tracers, boundary conditions derived from CAMS should be used. When possible, boundary conditions from the global CO2MVS IFS model will be used.

Emissions of greenhouse gasses and potential reactive gases are provided from respective emission inventories for each test case (described below). Therefore, all participants should at least include CO₂ in their simulations, with CH₄ being an optional second trace gas. In case chemistry is included, NO₂ and NO_x should also be simulated, e.g. to compare to TROPOMI satellite observations.

4.2 Rotterdam

Rotterdam is the second largest city in the Netherlands located on the south-west coast of the country. It is part of the Randstad area (area comprised of: Amsterdam, Rotterdam, The Hague and Utrecht) which holds about half of the total Dutch population. Furthermore, the Port of Rotterdam, which is located on the westernmost part of the city, is the largest seaport in Europe. Figure 4.1 shows the city of Rotterdam and the surrounding area with the simulated CO₂ plumes at 10 m height on 02.09.2022, 12:32 UTC.

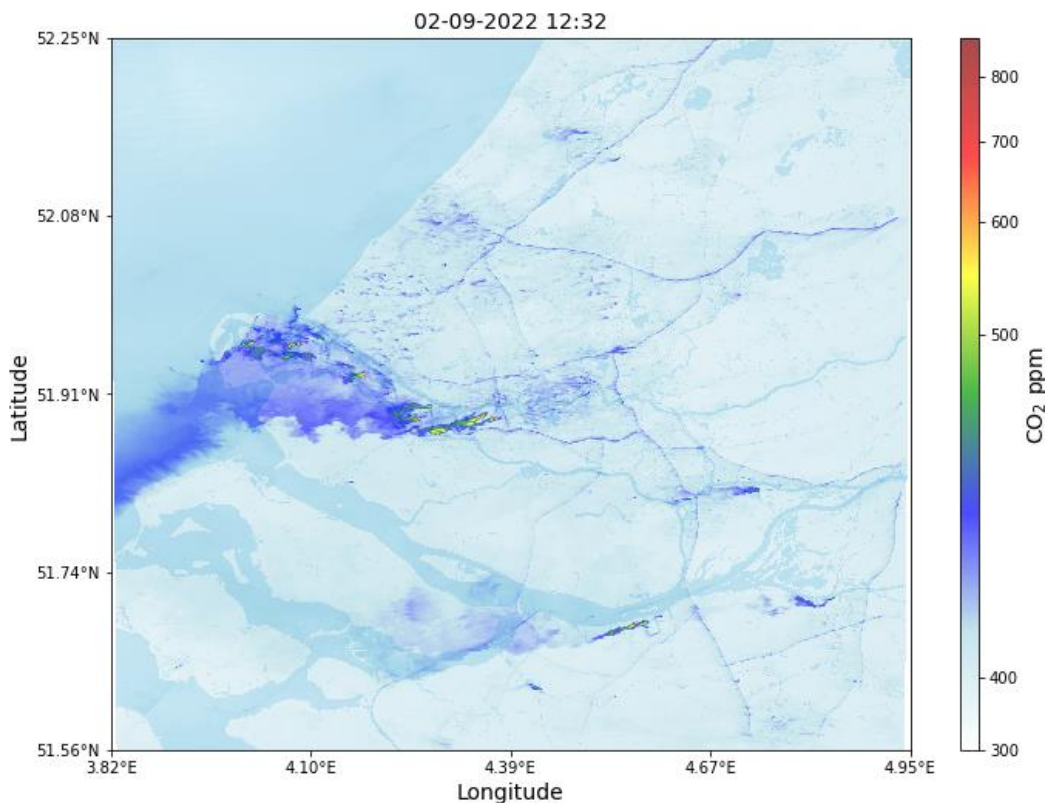


Figure 4.1: The CO₂ plume from Rotterdam, Rotterdam harbor and surrounding area. The CO₂ mole fraction at 10 m height, simulated with the MicroHH model is plotted.

Simulation specifications

a) Simulation days choice

The Rotterdam simulations will focus on the period 22.08.2022 to 02.09.2022 during which the intensive measurement campaign RITA2022 was conducted in the city. We recommend 23.08.2022 and 02.09.2022 as two mandatory simulation days.

The first day was chosen because the westerly winds were carrying the Rotterdam plume towards the Cabauw supersite measurement location. On this day the wind is coming from the sea which makes the incoming air relatively clear of possible plumes outside of the simulation domain.

One of the validation datasets for this case study is TROPOMI NO₂ data. Due to (partly) cloudy conditions for most of the campaign, we also recommend 02.09.2022 as the mandatory simulation day since the city plume is well visible in the TROPOMI data (Figure 4.2).

The first day (23.08.2022) was characterized with low to moderate westerly and south-westerly surface wind. Figure 4.3, leftmost panels, show wind direction and speed at three different measurement stations. It is visible that the wind speed and direction were consistent with each other at all three locations during most of the day with some variation during the night at the location furthest from the coast (Rotterdam locatie 06t). For all three locations the wind was the strongest around noon after which it gradually decreased and slowly turned from westerly

CATRINE

to south-westerly. Temperature and relative humidity (Figure 4.3, rightmost panels) indicate a warm day with sufficient moisture available for cloud formation.

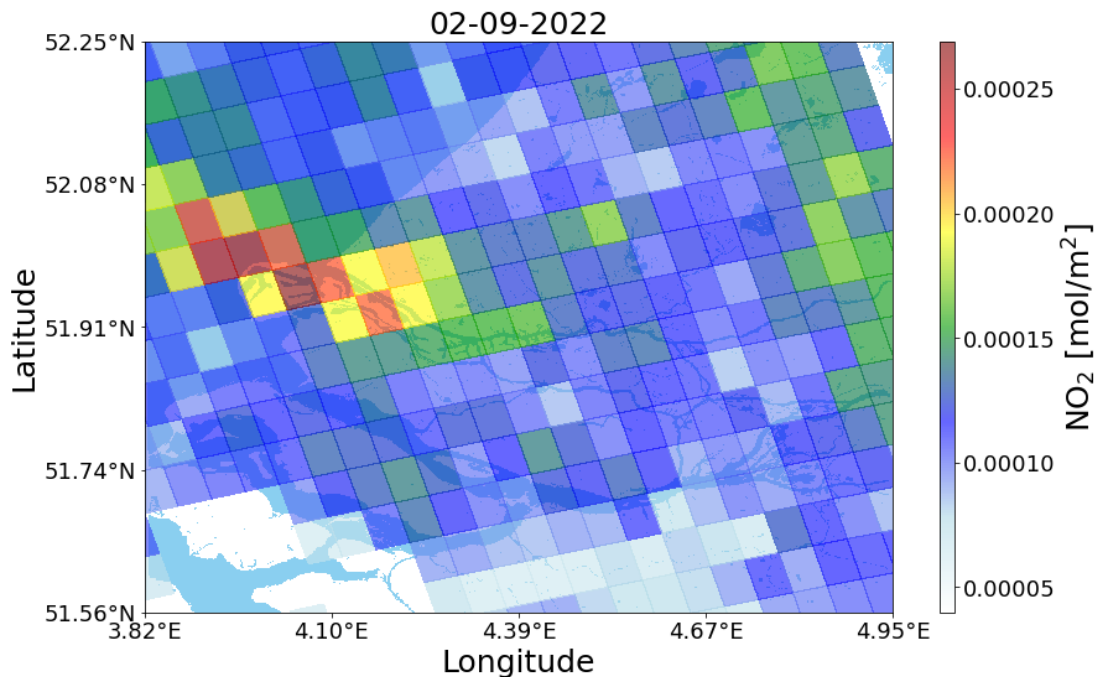


Figure 4.2 NO₂ total column concentrations as seen with the TROPOMI instrument above Rotterdam on 2-9-2022. TROPOMI overpass time was 12:32 UTC .

The second (02.09.2022) simulation day is characterized by moderate south-easterly and easterly surface wind. As seen in Figure 4.4, leftmost panels, this wind varied in strength throughout the day at locations further from the river and the sea where surface friction is larger. At locations closer to the river and the sea the winds remained relatively constant. The surface temperature and relative humidity (Figure 4.4, rightmost panels) indicate a warm and dry day with little potential for cloud formation which is confirmed by the clear TROPOMI image (Figure 4.2). Locations in which these measurements are available are given in Figure 4.5.

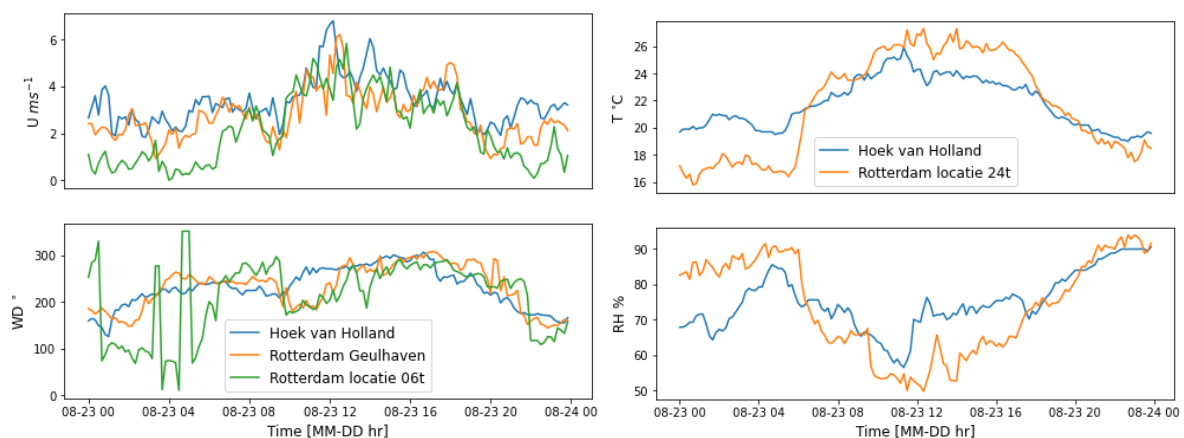


Figure 4.3 (left) Wind speed and direction and (right) temperature and relative humidity at two/three KNMI weather stations in the simulation domain on 23-08-2022.

CATRINE

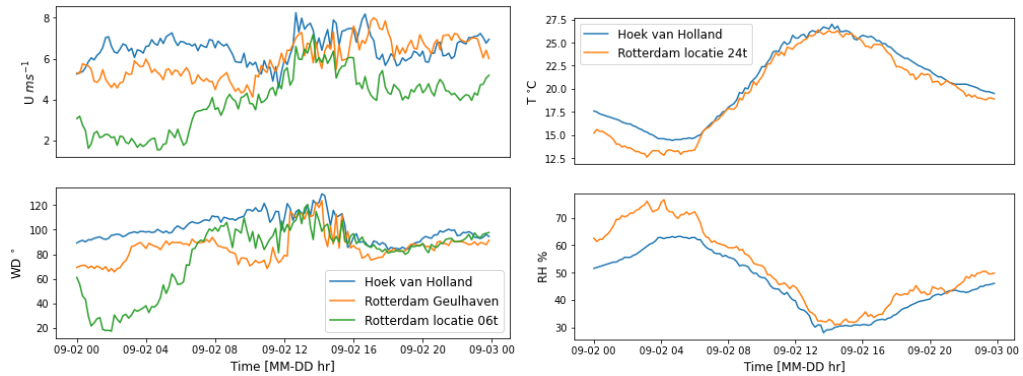


Figure 4.4 (left) Wind speed and direction and (right) temperature and relative humidity at three KNMI weather stations in the simulation domain on 02-09-2022.

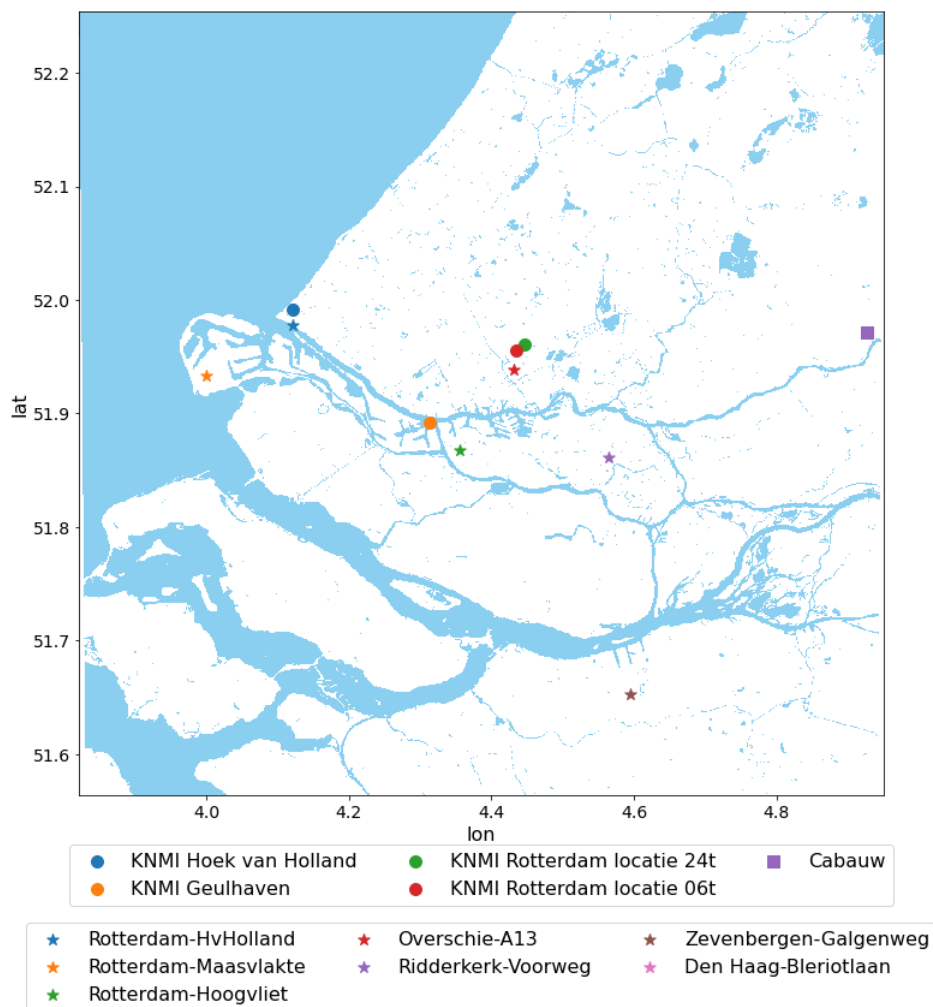


Figure 4.5 Locations of the KNMI weather stations, wind lidar from RITA2022 campaign and Luchtmeetnet air quality stations.

Figure 4.6 gives an overview of NO_2 measurements at multiple locations (Figure 4.5) in and around the city for both days. At the surface, we observe a consistent diurnal cycle that is linked with the temporal emission distribution (rush hour) and the dynamics of the boundary layer. Interestingly, for 02.09.2022, at the TROPOMI overpass time (12.30), the highest

CATRINE

concentrations are found within the plume observed by TROPOMI (Figure 4.2). Conversely, for 23.08.2022, higher concentrations are found at the one location east of the city center (Ridderkerk-Voorweg).

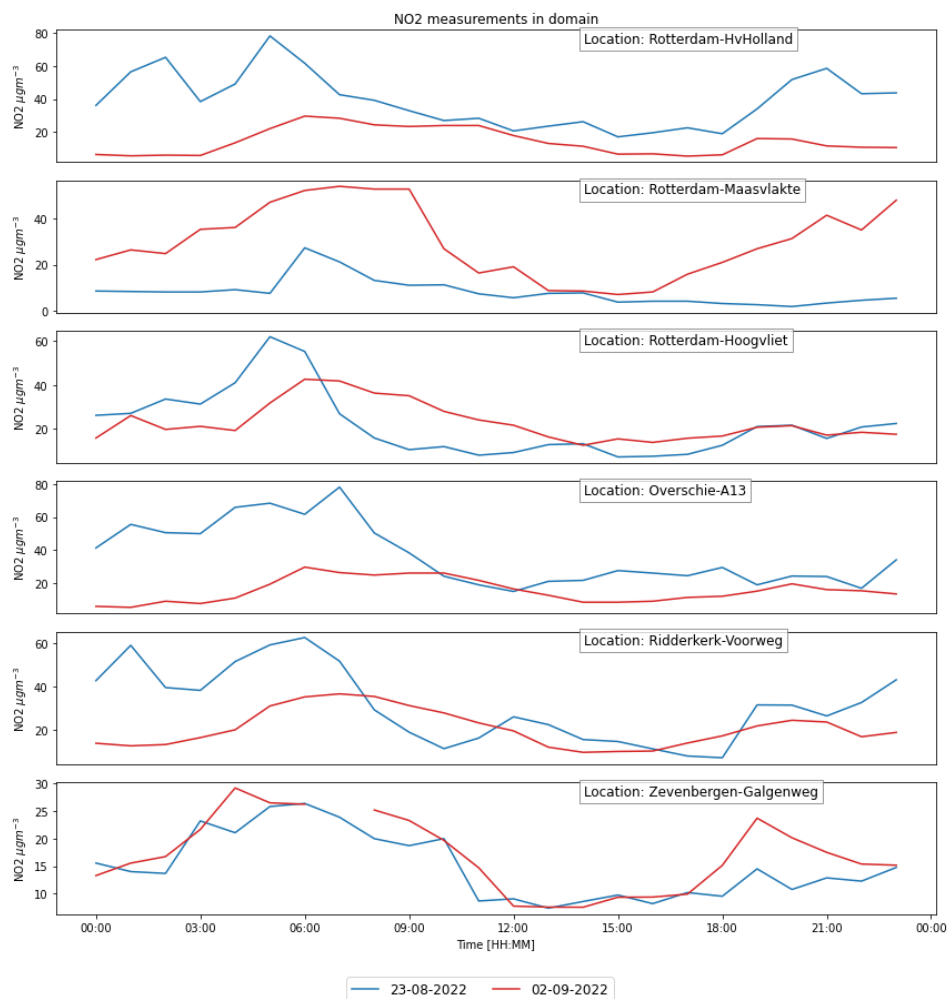


Figure 4.6 Hourly NO₂ measurements at ground level from Luchtmeetnet stations around the Rotterdam area and in the city.

b) Resolution and boundary conditions

The simulation domains should be centered in the Rotterdam city center with (51.909°N, 4.386°E). Figure 4.1 shows the recommended simulation domain with size of 76.8 x 76.8 km², centered around the Rotterdam city center.

We leave the definition of land surface boundary conditions to each individual model. However, if necessary, high-resolution data (elevation map, soil types, land-use) is available for the Rotterdam area, and specifics can be found in table A1 in Appendix A.

The following sections describe: (4.2.1) datasets containing information on emissions in the simulation domain (to be used as boundary conditions) and (4.2.2) measurements available for meteorology, GHGs, reactive species in the Rotterdam area. All described datasets will be shared with the participants as NetCDF-4 files, which list for instance times and locations of the measurement set.

4.2.1 Emissions

Surface fluxes

Surface emissions are provided as a bottom boundary condition and are available as hourly input. If supported by the model emissions are interpolated in time. Currently, two emissions inventories are used to assign a surface flux to a grid point (Table 4.2):

Table 4.2 Inventories providing surface fluxes for the Rotterdam simulation.

Dataset	Description	Source
TNO inventory	CH ₄ , CO ₂ , CO, pm2.5, NO and NO ₂ (as NO _x). 50x50 m ² resolution.	Not publicly available, internally shared with CATRINE partners.
Emissieregistratie	Dutch government's publicly available emission inventory for various compounds. 1x1 km ² resolution, used when TNO is unavailable.	link

Note that since TNO's inventory is not publicly available and will be internally shared with the participants, the inventory should be used only for the purpose of intercomparison and is not to be distributed further.

Point sources

Point sources are implemented from the Dutch government database [Woo-eMJV](#). Point sources for CH₄, CO₂, CO, NO and NO₂ (as NO_x) are described by their spatial position (lat, lon, height (or preferred height range)) and the strength of the source. Modelers can decide to pre-disperse the emissions to avoid numerical instabilities. Due to sparsity of the information on the heat content of the individual source in the Woo-eMJV database, we will assume currently no plume rise. With the MicroHH model, we will perform sensitivity simulations with various plume rise assumptions. We also assume that the emission strength of the sources is constant in time.

4.2.2 Validation datasets

Following observations are available for model validation:

Meteorology

RITA2022 campaign

During the RITA2022 campaign various measurements of meteorological conditions were taken at different locations throughout the city. Table 4.3 provides the overview of locations and measured variables.

Table 4.3 Overview of meteorological measurements during the RITA2022 campaign.

Measurement type	Location
Ceilometer (boundary layer height)	Rotterdam The Hague Airport, (51.9594°N, 4.44224° E)
	Rotterdam City Centre, (51.9199° N, 4.4710° E)
	Rotterdam De Slufter, (51.9336° N, 4.0000° E)

CATRINE

Wind lidar	Rotterdam City Centre, (51.9258 ° N, 4.4661 ° E)
Vaisala weather station (wind speed and direction, specific humidity, temperature, pressure)	Rotterdam Evides, (51.9061 ° N, 4.5354 ° E)

KNMI weather stations

There are three automatic weather stations in the domain operated by the Dutch weather institute (KNMI). Table 4 gives an overview of their locations and data available.

Table 4.4 Automated weather stations in the simulation domain.

Station	Measurements	Location
Hoek van Holland	U, WD, T, Tdew	(51.9911 ° N, 4.1217 ° E)
Geulhaven	U, WD	(51.8919 ° N, 4.3125 ° E)
Rotterdam airport locatie 06t	U, WD, T, Tdew	(51.9559 ° N, 4.43494 ° E)
Rotterdam airport locatie 24t	U, WD, T, Tdew	(51.9606 ° N, 4.4469 ° E)
Cabauw	U, WD, T, Tdew	(51.971 ° N, 4.927 ° E)

Here, U [m s^{-1}] is the mean horizontal wind, WD [°] is the wind direction, T [°C] is temperature and Tdew [°C] is the dewpoint temperature.

Greenhouse gasses

RITA2022

Table 4.5 gives an overview of greenhouse gas measurements taken during the RITA2022 campaign.

Table 4.5 Overview of air quality measurements during the RITA2022 campaign.

Measurement type	Location
Total column measurements (CO_2)	(51.982°N, 4.223°E), (51.926°N, 4.479°E), (51.964°N, 4.394°E) (operated by IUP)
	(51.934°N, 4°E) (operated by KIT)
	(51.906°N, 4.535°E) (operated by VU)
Point measurements (GHG + chemistry)	Rotterdam Evides, (51.9061°N, 4.5354°E)
Cabauw (GHG)	(51.971 °N, 4.927 °E)
Airborne (UAV, airplanes)	Data time dependent (netcdf file)
Ground mobile (GHGs, aerosols)	Data time dependent (netcdf file)

TROPOMI

CATRINE

TROPOMI instrument is placed aboard the Sentinel-5P satellite which takes daily snapshots of the atmosphere along its circumpolar orbit (Local overpass time ~1:30 PM). We will mostly focus on the total tropospheric column in the TROPOMI product, but CO, CH₄, and HCHO columns are also available for analysis. The overpass times for each day of the RITA2022 campaign are given in the table 4.6.

Table 4.6 TROPOMI overpass times for Rotterdam.

Campaign day	Overpass time (UTC)
22.08.2022	12:38
23.08.2022	12:19
24.08.2022	13:41
25.08.2022	13:22
26.08.2022	13:03
27.08.2022	12:44
28.08.2022	12:25
29.08.2022	12:07
30.08.2022	11:48
31.08.2022	11:29
01.09.2022	12:50
02.09.2022	12:32

Reactive gasses

Dutch air quality network

In case chemistry is included in the simulations, the Dutch air quality monitoring network, Luchtmeetnet, is available for validation. Table A2 in Appendix A provides an overview of measurement stations (their locations and species measured) which are in and around Rotterdam.

The data is explained on the Luchtmeetnet [website](#). However, as with all the above-mentioned datasets, locations and measurement data are available to the participants as a NetCDF file.

4.3 Paris

Choosing Paris and the Île-de-France region for a simulation case offers several advantages, including a rich data environment for both meteorological and GHG measurements, a complex urban area, and significant ongoing research including high-resolution modeling activities. Paris is one of the densest cities in Europe, with a population of over 2 million in the city and more than 12 million in the Île-de-France region. This density creates a complex network of greenhouse gas (GHG) emissions sources: transport, residential heating, commercial energy use, and industrial emissions, making it a perfect case study for urban emissions models. Additionally, Paris and the Île-de-France region benefit from a well-established GHG and meteorological monitoring network ([ICOS-Cities](#), [Urbisphere](#)) and extensive historical emission data from the Climate and Air Quality agency of Paris ([AirParif](#)), allowing for accurate model validation and a deeper understanding of emission trends over time.

4.3.1 Simulation configurations

a) Simulation period

The Paris simulations will focus on the period from January 10th to 20th, 2024, as this timeframe aligns with the availability of various data sources for validation, including measurements from the Total Carbon Column Observing Network (TCCON), LIDAR systems deployed for the URBISPHERE project, and a unique network of multiple Midcost CO₂ sensors.

b) Domain's configurations

The simulation domains should be centered in the Paris city center with latitude=48.866°N and longitude=2.333°E. The following table represents the characteristic of each domain in the WRF-LES model. For the inter-comparison, the high-resolution domain (D05) will be the target for simulations with MicroHH and PALM.

Table 4.7: WRF domains configurations

5 nested domains	D01	D02	D03	D04-LES	D05-LES
Horizontal resolution (m)	8100	2700	900	300	100
Grid number	212 x 212	262 x 262	250 x 250	358 x 358	466 x 466
Topography data (arc-second)	GMTED 30		SRTM 3		SRTM 1
Land use data (arc-second)	MODIS 30		CORINE 3		
Vertical level	51				

We define the LES domain to encompass the entire urban and suburban areas of Paris, ensuring that all CO₂ measurements stations (to validate the simulation) are within the D05-LES domain, as illustrated in the Figure 4.7. This domain has been carefully delineated to provide a comprehensive coverage of the city's atmospheric conditions and accurately representation of the spatial distribution of the data collected.

CATRINE

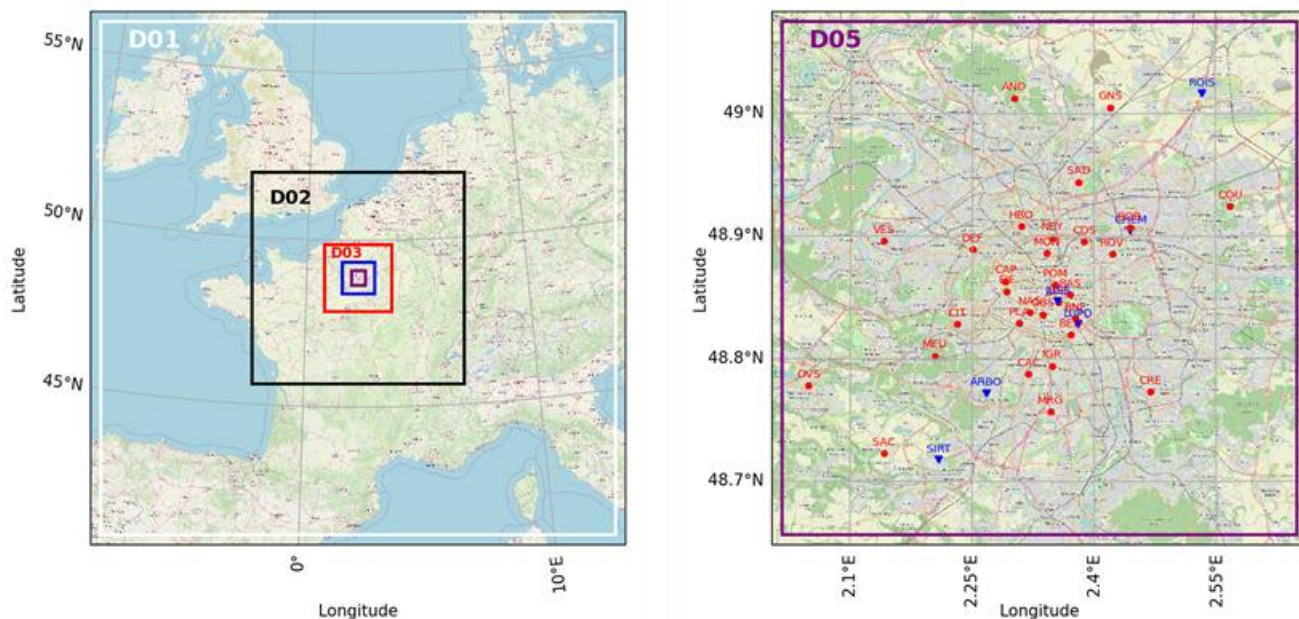


Figure 4. 7: WRF domains configuration. The red dots represent CO₂ and XCO₂ in-situ station locations, while the blue triangles denote wind lidar profiler positions.

c) Input data

To enhance the accuracy of WRF simulations, using high-resolution topography and land use/land cover (LULC) data provides a more detailed representation of terrain features and surface properties. This improves the modeling of small-scale atmospheric phenomena, surface-atmosphere interactions, and GHG emissions. Additionally, one of the goals is resolution matching, as when running WRF in LES mode, the input data should match the simulation resolution for optimal performance. It is generally better to have topography and LULC data that match or are closer in resolution to the model grid. This ensures that the model can capture the fine-scale features and interactions that drive local weather patterns and GHG dispersions

Topography: High-resolution topography datasets will be used for the high-resolution simulation in LES mode, including Shuttle Radar Topography Mission data at 3-arcsecond (SRTM 3) and 1-arcsecond (SRTM 1) resolutions, while Global Multi-resolution Terrain Elevation Data (GMTED) at 30-arcsecond resolution will be used for the domains at lower resolution.

Land use / Land cover: High-resolution land use/land cover datasets will be used, with CORINE data at 3-arcsecond resolution for the LES mode and the domain at 900m resolution, while MODIS data at 30-arcsecond resolution will be used for the lower resolution domains (Figure 4.8).

Input Meteorological data are sourced from ERA5, featuring approximately 25 km spatial resolution and 1-hour temporal resolution.

Boundary conditions for emissions are derived from CAMS (Copernicus Atmosphere Monitoring Service) data.

Emissions inventories are currently derived from two key sources: TNO and Airparif. These inventories are utilized to allocate surface fluxes to grid points within the model. The following table 4.8 provides a detailed description of the data sources and their respective characteristics.

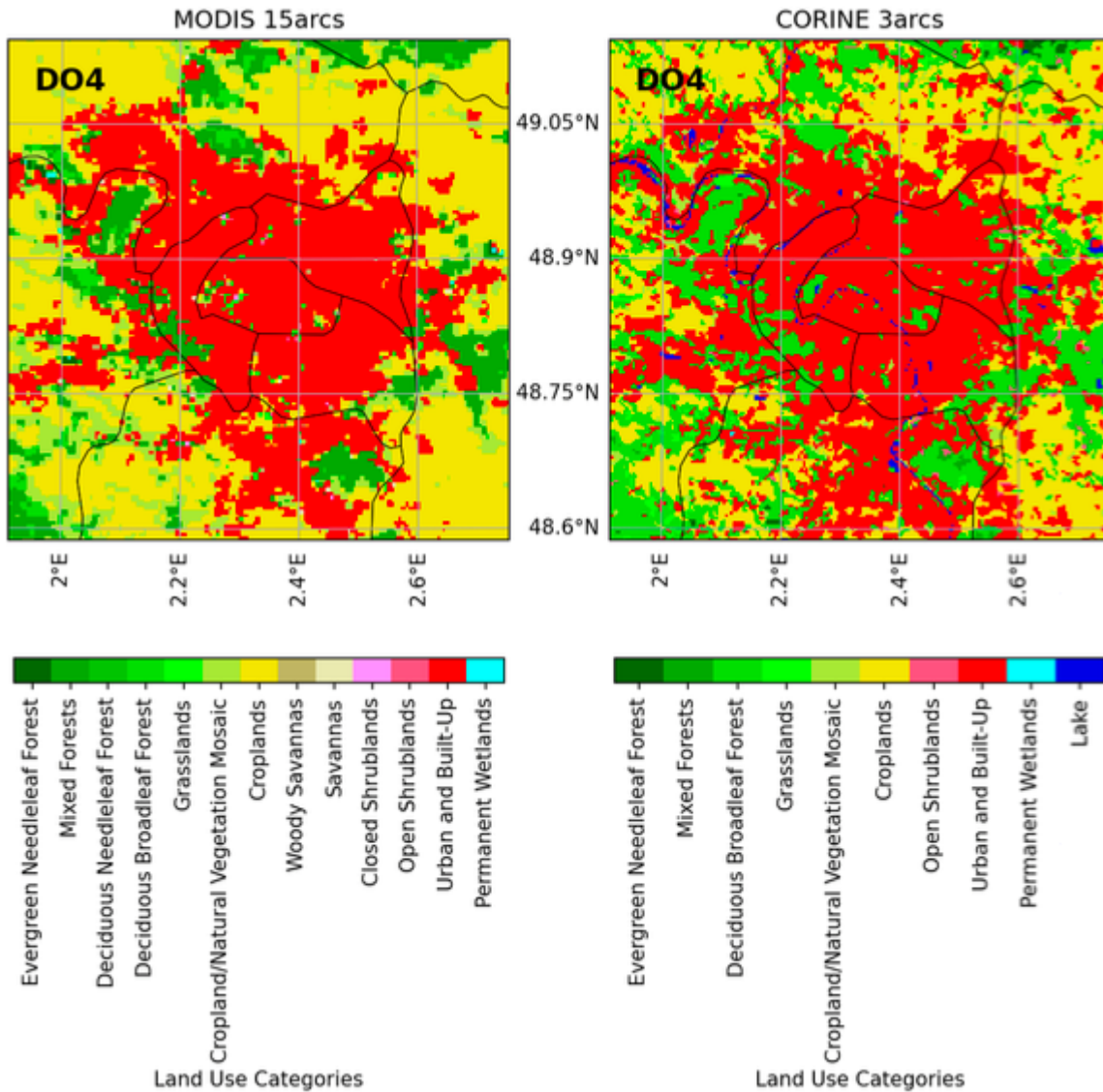


Figure 4.8: Map of the Land Use category from MODIS (left panel) and from CORINE (right panel) used for high-resolution simulations over Paris and the surrounding areas

Table 4.8: Inventories sources for the Paris simulation

Dataset	Description	Source
TNO	CH ₄ , CO ₂ , CO, and NO _x at 1x1 km ² resolution.	
Airparif	NO _x , CO ₂ , CO and Black Carbon at 500 x 500 m ² resolution.	Not publicly available, internally shared with CATRINE partners

4.3.2 Validation datasets

a) LIDAR: wind profiles

During the URBISPHERE project, 6 stations were deployed across Paris and Île-de-France to measure the profile of wind speed and directions (Table 4.9, Figure 4.9). The data are available in netcdf format.

Table 4. 9: Location of the lidar stations

Station Code	Station Name	Latitude (°)	Longitude (°)	Height MSL (m)	Height AGL (m)
ROIS	Aéroport Roissy-Charles-de-Gaulle	49.016	2.53366	112	4
CHEM	Chemin Vert Bobigny	48.9046	2.4447	98	52
JUSS	Tour Zamansky Jussieu	48.8469	2.3555	125	88
LUPD	LISA Université Paris Diderot	48.8278	2.38064	65	26
ARBO	Arboretum de la Vallée-aux-Loups	48.7717	2.26769	99	1
SIRT	Observatoire SIRTÀ	48.7173	2.20887	154	0

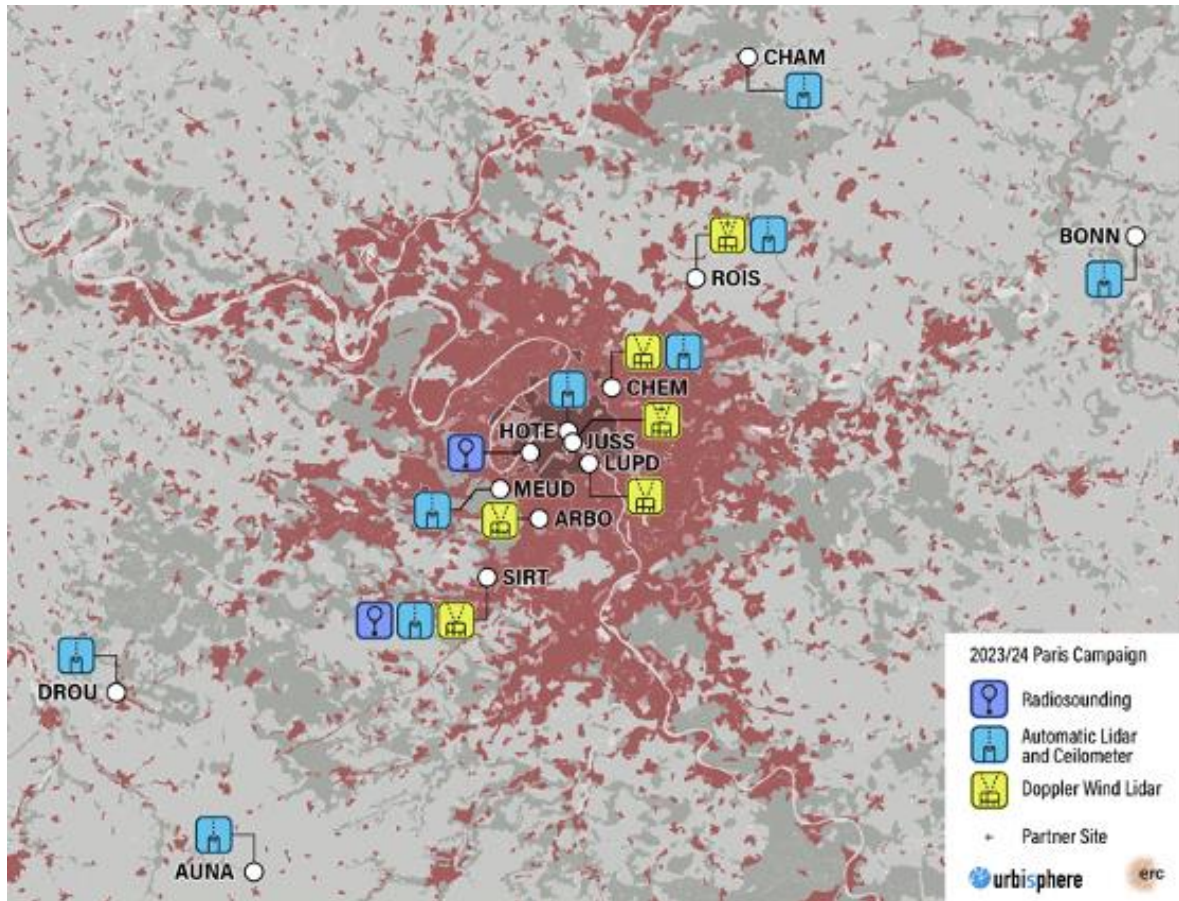


Figure 4.9: Map of the deployed Doppler Wind Lidars and Ceilometers during the selected period as part of the Urbisphere project (courtesy of A. Christen, Univ. Of Freiburg)

b) Total column measurement

- **Total Carbon Column Observing Network (TCCON):** the station is in the center of Paris, at Sorbonne Université, Campus Pierre et Marie Curie, 4 Place Jussieu, Paris 05, France (48.85 N, 2.36 E). Data in netCDF format are publicly available (<http://tccon.org/>).
- **EM27:** Currently we have access to data from two EM27 stations, located at Gonesse (48.991°N, 2.445°E) and Saclay (48.711°N, 2.148°E).

c) Paris Mid-cost CO₂ sensor network

As part of the ICOS-Cities project, a network of **over 25 mid-cost CO₂ sensors** has been strategically installed throughout the urban and suburban areas of Paris (Figure 4.10, Table 4.10).

CATRINE

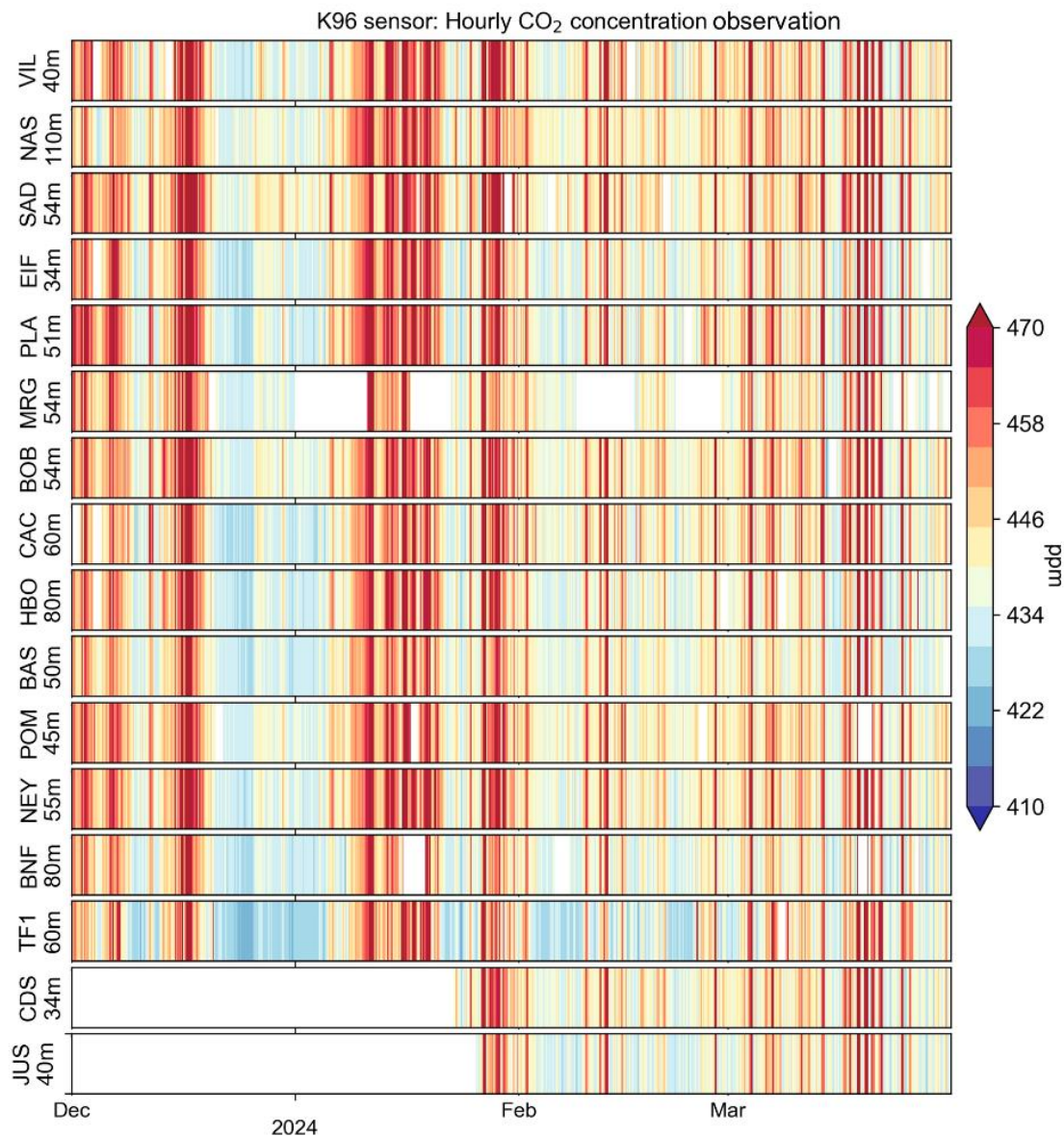


Figure 4.10: Measured mole fractions (ppm) by the Paris CO₂ mid-cost sensor network in late 2023 and early 2024 (O. Laurent, M. Ramonet, M. Chariot, courtesy of LSCE).

Table 4.10: Location of the different CO₂ stations

Station code	Latitude (°)	Longitude (°)	Height AGL (m)
ATC	48.71	2.1475	10
VIL	48.9349	2.3357	40.5
NAS	48.8383	2.3213	110
TF1	48.8340	2.2604	60
CDS	48.8953	2.3870	34
CAC	48.7887	2.3203	60
SAD	48.9442	2.3813	54

CATRINE

NEY	48.8992	2.3487	55
BAS	48.8524	2.3704	50
BOB	48.9077	2.4445	54
MRG	48.7569	2.3463	54
BNF	48.8334	2.3774	80
PLA	48.8300	2.3077	51
HBO	48.9080	2.3105	80
JUS	48.8464	2.3561	40
EIF	48.8554	2.2926	34.5
POM	48.8612	2.3525	45
HMO	48.7976	2.4528	100
MEU	48.802459	2.2043633	45, 65, 90
SAC	48.723	2.142	15, 60, 100
ROV	48.885674	2.4223371	103
CIT	48.828333	2.2313888	88
AND	49.0126	2.3018	60
OVS	48.7779	2.0486	20
GNS	49.0052	2.4205	5
VES	48.896028	2.1414607	40
CRE	48.773277	2.4692909	37
DEF	48.889228	2.2505837	165
IGR	48.794204	2.3480769	surface

5 Simulation protocol

To make the model intercomparison as easy as possible, the model output should be stored and delivered in a standardized format. All data should be delivered in NetCDF-4 file format with dimensions as described in table 5.1.

Table 5.1 Overview of NetCDF dimensions.

Name	Details
longitude	Number of grid points in zonal direction
latitude	Number of grid points in meridional direction
level	Number of full (cell center) vertical level
levelh	Number of half (cell edge) vertical levels
time	Number of timesteps

5.1 Data output

Data should be delivered as time series with spatial dimensions varying if 1-, 2- or 3-D transect is being recorded. Table 5.2 gives an overview of variables, units and dimensions which should be delivered per each simulation.

Table 5.2 Overview of variables, units and dimensions that should be recorded in the output files.

Name	Details	Units	Dimensions
u	Eastward wind	m s^{-1}	time, level, latitude, longitude
v	Northward wind	m s^{-1}	time, level, latitude, longitude
w	Vertical velocity	m s^{-1}	time, level, latitude, longitude
e	Turbulent kinetic energy	m^2s^{-2}	time, level, latitude, longitude
T	Air temperature	K	time, level, latitude, longitude
qt	Specific humidity	kg kg^{-1}	time, level, latitude, longitude

CATRINE

co2	CO_2 dry air mole fraction	mol mol ⁻¹	time, level, latitude, longitude
ch4 (optional)	CH_4 dry air mole fraction	mol mol ⁻¹	time, level, latitude, longitude
tracer (optional)	Chemical tracer dry air mole fraction	mol mol ⁻¹	time, level, latitude, longitude

- 1D - vertical profiles are taken at a defined (lat, lon) position in the domain which corresponds to point measurements in each simulation case. The vertical transects should be taken for every measurement location provided with (lat, lon) in the simulation case description for both meteorology and air quality validation datasets (including the total column measurements). The sampling frequency should be 1 minute.
- 2D - horizontal cross-sections through the whole domain should be recorded with frequency of 5 minutes. Variables should be recorded at : [10, 30, 50, 70, 90, 110, 500, 1000, 2000] m at the native grid resolution.
- 3D - 3D snapshots of the domain should be recorded every 15 minutes at the native grid resolution.

5.2 Non-standard data output

Mobile data

In case mobile measurements (ground based, aircraft or UAV) are available for validation, the simulation needs to be sampled in a way that mimics the movement of the measurement device. In other words, (lat, lon, height) of the measurement is also time dependent and should correspond with the (lat, lon, height, time) provided in the validation dataset.

TROPOMI

TROPOMI output corresponds to vertically integrated concentrations in the domain. Due to the need for using the vertical averaging kernel, we will use the 3D snapshot closest to the TROPOMI overpass time for each case.

Total column measurements (EM27)

It was indicated in the previous section that for total column measurements, the vertical profiles through the domain at the location of the measurement device should be delivered. Because total columns are measured by angling the device directly into the Sun which varies throughout the day, we leave the data delivery for this measurement devices open for discussion.

6 Appendix A (Rotterdam)

In this appendix tables containing additional information on datasets used for the Rotterdam simulation can be found.

A.1 Land surface

Table A1 Datasets used to create surface boundary conditions for Rotterdam in MicroHH.

Dataset	Description	Source
TOP10NL	High-resolution (10x10 m ²) land-use data	link
Bofek2012	High-resolution (10x10 m ²) soil types and properties in the Netherlands	link
AHN	Elevation map (5x5 m ² or 0.5x0.5 m ²), used for building drag calculation	link

Note that both Bofek2012 and TOP10NL are originally vector datasets that were gridded to 10 m resolution that can be shared with other participants.

A.2 Air quality stations

Table A2 Locations and list of species measured at automated Luchtmeetnet air quality stations that fall into the simulation domain for Rotterdam.

Location	Number	Latitude	Longitude	Components
Overschie-A13	NL01491	51.93858	4.43070	FN, NO, NO ₂ , PM ₁₀ , PM ₂₅ , BCWB
Rotterdam-Maasvlakte	NL01497	51.93352	3.99972	NO ₂ , NO, LKI, PM ₁₀ , PM ₂₅
Rotterdam-HvHolland	NL01496	51.97780	4.12194	C ₆ H ₆ , C ₇ H ₈ , FN, NO, NO ₂ , O ₃ , PM ₁₀ , PM ₂₅ , SO ₂ , BCWB
Ridderkerk-Voorweg	NL01912	51.86173	4.56381	NO ₂ , PM ₁₀ , PM ₂₅
Rotterdam-Hoogvliet	NL01485	51.86742	4.35524	C ₆ H ₆ , C ₇ H ₈ , NO, NO ₂ , O ₃ , PM ₁₀ , SO ₂ , PM ₂₅

CATRINE

Ridderkerk-A16	NL01489	51.86942	4.58007	NO, NO2, PM10, PM25
Zevenbergen-Galgenweg	NL53016	51.65321	4.59488	C6H6, C7H8, C8H10, NO, NO2, PM10, PM25
Den Haag-Rebecquestraat	NL10404	52.07715	4.28919	NO, NO2, O3, PM10, PM25
Den Haag-Amsterdamse Veerkade	NL10445	52.07507	4.31587	NO, PM10, NO2
Fijnaart-Zwingelspaansedijk	NL10246	51.65373	4.51527	NO, PM10, NO2
Strijensas Buitendijk	NL53020	51.7134	4.58325	C6H6, C7H8, C8H10, NO, NO2, PM10, PM25
Zierikzee-Lange Slikweg	NL10301	51.63471	3.91662	NO, NO2, O3
Moerdijk-Julianastraat	NL53004	51.69941	4.62371	C6H6, C7H8, C8H10, FN, NO, NO2, PM10, PM25
Rotterdam-Geulhaven	NL01484	51.889	4.31250	C6H6, C7H8, SO2
Rotterdam-Statenvweg	NL01493	51.92711	4.46136	FN, NO, NO2, O3, PM10, PM25, BCWB
Schiedam-A.Arienstraat	NL01494	51.92139	4.40139	C6H6, C7H8, FN, NO, NO2, O3, PM10, PM25, PS, BCWB
Dordrecht-Bamendaweg	NL10442	51.80066	4.70824	NO, NO2, O3, PM10
Zegveld-Oude Meije	NL10633	52.13795	4.83819	FN, NH3, NO, NO2, O3, PM10
Westmaas-Groeneweg	NL10437	51.78658	4.45053	NO, NO2, O3, PM10
Breda-Bastenakenstraat	NL10241	51.60308	4.78102	NO, NO2, O3, PM10, PM25
Den Haag-Bleriotlaan	NL10446	52.03902	4.35938	NO, NO2, O3, PM10
Cabauw-Wielsekade	NL10644	51.97449	4.92330	NO, NO2, O3, PM10, PM25, SO2, BC
Rotterdam-Schiedamsevest	NL10418	51.91423	4.47992	NO, NO2, O3, PM10, PM25
Breda-Tilburgseweg	NL10240	51.59353	4.82494	NO, NO2, PM10, PM25

CATRINE

Klundert-Kerkweg	NL53015	51.66894	4.54166	PM25, C6H6, C7H8, C8H10, NO, NO2, PM10
Rotterdam-Pleinweg	NL01487	51.89113	4.48066	FN, NO, NO2, PM10, PM25, BCWB
Rotterdam-Zwartewaalstraat	NL01488	51.89361	4.48759	FN, NO, NO2, PM10, PM25, BCWB
Maassluis-Kwartellaan	NL01495	51.93207	4.22780	C6H6, C7H8, NO, NO2, O3, PM10, PM25, SO2
Vlaardingen-Riouwlaan	NL10449	51.91488	4.32943	NO, NO2, O3, PM10, PM25
Den Haag-Neherkade	NL10450	52.06254	4.31855	NO2, NO, PM10, NOx, O3, PM2.5, PM25

7 References

- Basu, S. et al. (2018). The impact of transport model differences on CO₂ surface flux estimates from OCO-2 retrievals of column average CO₂, *Atmos. Chem. Phys.*, 18, 7189–7215, <https://doi.org/10.5194/acp-18-7189-2018>.
- V. Beck, T. Koch, R. Kretschmer, J. Marshall, R. Ahmadov, C. Gerbig, D. Pillai, et al. “The WRF Greenhouse Gas Model (WRF-GHG)”. (2012).
- Chulakadabba, A., Sargent, M., Lauvaux, T., Benmergui, J. S., Franklin, J. E., Chan Miller, C., Wilzewski, J. S., Roche, S., Conway, E., Souri, A. H., Sun, K., Luo, B., Hawthorne, J., Samra, J., Daube, B. C., Liu, X., Chance, K., Li, Y., Gautam, R., Omara, M., Rutherford, J. S., Sherwin, E. D., Brandt, A., and Wofsy, S. C. (2023): Methane point source quantification using MethaneAIR: a new airborne imaging spectrometer, *Atmos. Meas. Tech.*, 16, 5771–5785, <https://doi.org/10.5194/amt-16-5771-2023>
- Alexandre Danjou, Grégoire Broquet, Jinghui Lian, François-Marie Bréon, Thomas Lauvaux (2024): Evaluation of light atmospheric plume inversion methods using synthetic XCO₂ satellite images to compute Paris CO₂ emissions, *Remote Sensing of Environment*, Volume 305, <https://doi.org/10.1016/j.rse.2023.113900>
- Deardorff, J.W., (1980). Stratocumulus-capped mixed layers derived from a threedimensional model. *Boundary-Layer Meteorol.* 18, 495–527.
- Gaubert et al. (2019). Global atmospheric CO₂ inverse models converging on neutral tropical land exchange, but disagreeing on fossil fuel and atmospheric growth rate, *Biogeosciences*, 16, 117–134.
- Gaudet, BJ, et al 2017, Exploration of the impact of nearby sources on urban atmospheric inversions using large eddy simulation. *ElemSciAnth*, 5: 60. DOI: <https://doi.org/10.1525/elementa.247>
- Gronemeier, T. and Sührling, M., 2019. On the effects of lateral openings on courtyard ventilation and pollution—a large-eddy simulation study. *Atmosphere* 10 (2), 63
- van Heerwaarden, C. C., Van Stratum, B. J., Heus, T., Gibbs, J. A., Fedorovich, E., & Mellado, J. P. (2017). MicroHH 1.0: A computational fluid dynamics code for direct numerical simulation and large-eddy simulation of atmospheric boundary layer flows. *Geoscientific Model Development*, 10(8), 3145-3165.
- Hellsten, A., Ketelsen, K., Sührling, M., Auvinen, M., Maronga, B., Knigge, C., Barmpas, F., Tsegas, G., Moussiopoulos, N., Raasch, S., 2021. A nested multi-scale system implemented in the large-eddy simulation model PALM model system 6.0. *Geosci. Model Dev.* 14 (6), 3185–3214.
- Hersbach, H., Bell, B., Berrisford, P., Hirahara, S., Horányi, A., Muñoz-Sabater, J., ... & Thépaut, J. N. (2020). The ERA5 global reanalysis. *Quarterly Journal of the Royal Meteorological Society*, 146(730), 1999-2049.
- Inness, A., Ades, M., Agustí-Panareda, A., Barré, J., Benedictow, A., Blechschmidt, A. M., ... & Suttie, M. (2019). The CAMS reanalysis of atmospheric composition. *Atmospheric Chemistry and Physics*, 19(6), 3515-3556.
- Kanani, F., Träumner, K., Ruck, B. and Raasch, S. (2014). What determines the differences found in forest edge flow between physical models and atmospheric measurements? – an LES study. *Meteorol. Z.* 23, 33–49.
- Karttunen, S., Kurppa, M., Auvinen, M., Hellsten, A. and Järvi, L. (2020) . Large-eddy simulation of the optimal street-tree layout for pedestrian-level aerosol particle concentrations—A case study from a city-boulevard. *Atmos. Environ.* X 6, 100073.

CATRINE

- Khan, B., Banzhaf, S., Chan, E.C., Forkel, R., Kanani-Sühring, F., Ketelsen, K., Kurppa, M., Maronga, B., Mauder, M., Raasch, S., Russo, E., Schaap, M. and Sühring, M. (2021). Development of an atmospheric chemistry model coupled to the PALM model system 6.0: implementation and first applications. *Geosci. Model Dev. (GMD)* 14, 1171–1193.
- Matthäus Kiel, Anmarie Eldering, Dustin D. Roten, John C. Lin, Sha Feng, Ruixue Lei, Thomas Lauvaux, Tomohiro Oda, Coleen M. Roehl, Jean-Francois Blavier, Laura T. Iraci, (2021): Urban-focused satellite CO₂ observations from the Orbiting Carbon Observatory-3: A first look at the Los Angeles megacity, *Remote Sensing of Environment*, Volume 258, <https://doi.org/10.1016/j.rse.2021.112314>
- Krc, P., Resler, J., Sühring, M., Schubert, S., Salim, M. H., and Fuka, V. (2021). Radiative Transfer Model 3.0 integrated into the PALM model system 6.0. *Geosci. Model Dev.*, 14, 3095–3120.
- Krol, M., van Stratum, B., Anglou, I., & Boersma, K. F. (2024). Evaluating NO_x stack plume emissions using a high-resolution atmospheric chemistry model and satellite-derived NO₂ columns. *Atmospheric Chemistry and Physics*, 24(14), 8243-8262.
- Kurppa, M., Hellsten, A., Roldin, P., Kokkola, H., Tonttila, J., Auvinen, M., Kent, C., Kumar, P., Maronga, B. and Järvi, L. (2019). Implementation of the sectional aerosol module SALSA2. 0 into the PALM model system 6.0: model development and first evaluation. *Geosci. Model Dev.* 12, 1403–1422.
- Lauvaux T., et al. 2016, High-resolution atmospheric inversion of urban CO₂ emissions during the dormant season of the Indianapolis Flux Experiment (INFLUX), *J. Geophys. Res. Atmos.*, 121, 5213–5236, DOI: <https://doi.org/10.1002/2015JD024473>
- Letzel, M.O., Krane, M. and Raasch, S. (2008). High resolution urban large-eddy simulation studies from street canyon to neighbourhood scale. *Atmos. Environ.* 42, 8770–8784.
- Lilly, D. K. (1996). A comparison of incompressible, anelastic and Boussinesq dynamics. *Atmospheric research*, 40(2-4), 143-151.
- Lin and Gerbig, (2005): Accounting for the effect of transport errors on tracer inversions, *Geophys. Res. Lett.*, 32
- P. Mahadevan, S. Wofsy, D. Matross, X. Xiao, A. Dunn, J. Lin, C. Gerbig, et al., “A satellite-based biosphere parameterization for net ecosystem CO₂ exchange: Vegetation Photosynthesis and Respiration Model (VPRM)”, *Global Biogeochemical Cycles*, vol. 22, no. 2, (2008). DOI: <https://doi.org/10.1029/2006GB002735>
- Maronga, B., Banzhaf, S., Burmeister, C., Esch, T., Forkel, R., Fröhlich, D., Fuka, V., Gehrke, K.F., Geletic, J. and Giersch, S. (2020). Overview of the PALM model system 6.0. *Geosci. Model Dev.* 13, 1335–1372.
- Park, S.B., Baik, J.J., Raasch, S. and Letzel, M.O. (2012). A large-eddy simulation study of thermal effects on turbulent flow and dispersion in and above a street canyon. *J. Appl. Meteorol. Climatol.* 51, 829–841.
- Razak, A.A., Hagishima, A., Ikegaya, N. and Tanimoto, J. (2013). Analysis of airflow over building arrays for assessment of urban wind environment. *Build. Environ.* 59, 56–65.
- Ražnjević, A., van Heerwaarden, C., and Krol, M. (2022)a. Evaluation of two common source estimation measurement strategies using large-eddy simulation of plume dispersion under neutral atmospheric conditions, *Atmos. Meas. Tech.*, 15, 3611–3628, <https://doi.org/10.5194/amt-15-3611-2022>, 2022.
- Ražnjević, A., Van Heerwaarden, C., Van Stratum, B., Hensen, A., Velzeboer, I., Van Den Bulk, P., & Krol, M. (2022)b. Interpretation of field observations of point-source

CATRINE

- methane plume using observation-driven large-eddy simulations. *Atmospheric Chemistry and Physics*, 22(10), 6489-6505.
- Resler, J., Krc, P., Belda, M., Jurus, P., Benesova, N., Lopata, J., Vlcek, O., Damaskova, D., Eben, K., Derbek, P., Maronga, B. and Kanani-Sühring, F. (2017). PALM-USM v1.0: a new urban surface model integrated into the PALM large-eddy simulation model. *Geosci. Model Dev.* 10, 3635–3659.
- Schuh et al., 2019: Quantifying the impact of atmospheric transport uncertainty on CO₂ surface flux estimates, *Global Biogeochemical Cycles*, 33, 484–500
- Skamarock W. C., Klemp J. B., Dudhia J., Gill D. O., Liu Z., Berner J., Wang W., Powers J. G., Duda M. G., Barker D. M. et Huang X.-Y (2019). « A Description of the Advanced Research WRF Version 4 ». In : NCAR Tech. Note NCAR/TN-556+STR, 145pp. DOI: <https://doi.org/10.5065/1dfh-6p97>
- van Stratum, B. J. H., van Heerwaarden, C. C., & Vilà-Guerau de Arellano, J. (2023). The Benefits and Challenges of Downscaling a Global Reanalysis With Doubly-Periodic Large-Eddy Simulations. *Journal of Advances in Modeling Earth Systems*, 15(10), e2023MS003750.
- Stull, R. B. (2012). *An introduction to boundary layer meteorology* (Vol. 13). Springer Science & Business Media.
- Wicker, L.J. and Skamarock, W.C. (2002). Time-splitting methods for elastic models using forward time schemes. *Mon. Weather Rev.* 130, 2088–2097.
- Williamson, J.H. (1980). Low-storage Runge-Kutta schemes. *J. Comput.* 35, 48–56.

Document History

Version	Author(s)	Date	Changes
0.1	Anja Raznjevic, Bart van Stratum, Maarten Krol, Leena Järvi, Alohotsy Rafalimanana, Thomas Lauvaux, Charbel Abdallah	December 2024	Initial version
1.0	Maarten Krol, Thomas Lauvaux	December 2024	Revised after review comments

Internal Review History

Internal Reviewers	Date	Comments
M Diamantakis (ECMWF) and Stefan Versick (KIT)	December 2024	